Paleoclimates, 1998, Vol. 2(2–3), pp. 163–182
Reprints available directly from the publisher
Photocopying permitted by license only

CIRCULATION AND SEDIMENT TRANSPORT IN THE NORTH ATLANTIC DURING THE MELTWATER EVENT NEAR 13.5 KA B.P.

DAN SEIDOV[a,†] and BERND J. HAUPT[b,*]

[a]*Geologisch-Paläontologisches Institut, Universtät Kiel, Olshausenstr. 40 and*
[b]*Sonderforschungsbereich 313, Universität Kiel, Heinrich-Hecht-Platz 10, D-24118, Kiel, Germany*

(Received 20 January 1997; Revised 23 August 1997; In final form 15 September 1997)

The circulation, sedimentation and ventilation regime of the North Atlantic at present and at the last glacial maximum are addressed via numerical modeling for the meltwater event (MWE) near 13.5 ka B.P. The ocean general circulation model (OGCM) is driven by meltwater sea surface thermohaline conditions and wind stress. The MWE ocean circulation is compared to the control run based on the present day sea surface climatology. The output of the OGCM is then used in a sedimentation model and in a model to trace water parcel trajectories. The results of the sediment transport model and trajectory-tracing calculations both indicate essentially different circulation and deep ocean ventilation regime at the MWE as compared to the control run. The sedimentation model gives a lower sedimentation rate in the Nordic Seas and higher rate in the eastern North Atlantic at the MWE than at present. There is almost no MWE sediment deposition in the Gulf Stream area, and a lower rate than at present in the Caribbean. The circulation pattern and the trajectory-tracing model both indicate that these major changes of sediment transport are caused by disappearance of the southward flowing deep western boundary current. However, only the trajectory-tracing model clearly reveals the dramatic change of the ventilation regime caused by much shallower and southward shifted MWE convection. According to the model the deep ocean at the MWE was not ventilated at all — a result strongly supported by proxy-data analyses. The MWE subtropical pool of high potential vorticity is restricted to the western North Atlantic in sharp contrast to the spread of this pool over the entire subtropics today. At the MWE, the particles deployed at the surface in the convection regions never penetrated deeper than 1 km, whereas at present the downward transport at the deep convection sites is deeper than 2 km. Hence the trajectory-tracing calculations confirm the recent proxy-data analyses and Eulerian circulation modeling indicating that the most important ocean driving mechanism, namely the North Atlantic Deep Water outflow, was completely missing from the ocean system at the MWE.

Keywords: Ocean circulation, convection, Lagrangian particle tracing, meltwater event, sediment transport

* Corresponding author. E-mail: dseidov@essc.psu.edu;bernd@sfb313.uni-kiel.de.
† Present address: Earth System Science Center, Pennsylvania State University, 248 Deike, University Park, PA 16801, USA.

INTRODUCTION

At present, the world ocean thermohaline circulation is driven by the production of the North Atlantic Deep Water (NADW) in the northern North Atlantic (NA) and the Norwegian-Greenland Seas (NGS). The deep outflow of NADW initiates the global thermohaline conveyor (Gordon, 1986; Broecker and Denton, 1989; Schmitz, 1995), known also as 'salinity conveyor belt' (Broecker, 1991).

Proxy data analysis indicates that the Pleistocene NA conveyor operated differently from present, causing different modes of circulation (Boyle and Keigwin, 1987; Broecker and Denton, 1989; Broecker, 1991; Bond *et al.*, 1992; Lehman and Keigwin, 1992; Sarnthein *et al.*, 1994, 1995). Many numerical simulations of widely different complexity confirmed that multiple stable modes of a buoyancy-driven conveyor may indeed occur (*e.g.*, F. Bryan, 1986; Manabe and Stouffer, 1988, 1995; Marotzke and Willebrand, 1991; Wright and Stocker, 1991; Fichefet *et al.*, 1994; Rahmstorf, 1994, 1995; Stocker, 1994; Weaver and Hughes, 1994).

The last glacial maximum (LGM) near 18 ka B.P. has the best proxy-data coverage of any Pleistocene glaciation, and therefore this event has attracted most interest among modelers. However, although the LGM conveyor differed noticeably from its present-day analogue, the indeed dramatic circulation changes in the northern NA and NGS occurred at the first major postglacial meltwater event (MWE) near 13.5 ka B.P. in the NGS and north-eastern NA (*e.g.*, Sarnthein *et al.*, 1995). Based on the data from CLIMAP (1981), Duplessy *et al.* (1991) and Sarnthein *et al.* (1995), Seidov *et al.* (1996) use ocean surface modern climatology and paleo-reconstructions to simulate the present and past NA circulation pattern by means of an ocean general circulation model (OGCM). The model is driven by wind stress, and by the heat and freshwater fluxes calculated from specified sea surface temperature (SST) and sea surface salinity (SSS). The OGCM runs yield three-dimensional (3-D) temperature, salinity and velocity fields relevant to the present-day, the LGM and the MWE sea surface conditions.

Although an OGCM provides the ocean circulation pattern sufficient for the ocean climate analysis, there are some topics that cannot be addressed on a sole base of such simulations, for example ocean sediment transport. Moreover, visualization of the deep ocean ventilation and actual water motion meets some difficulties in traditional circulation modeling. Recently, we have recruited a major simulation technique, the OGCM, and two complementary models that quantify the sediment transport and visualize the true three-dimensional water motion. (For details of using the approach see Seidov and Haupt (1997); further referred as SH).

Typically, sedimentation records are employed to reconstruct ocean currents that cause observed sediment drifts. Provided that past circulation patterns differed from the modern velocity distribution, the paleo-sedimentation and particle transport had inevitably to be different. Many attempts have been made to infer the circulation pattern from sediment structure and especially from ice-rafted debris (Goldschmidt *et al.*, 1992; Honjo, 1990; Seibold and Berger, 1993, Goldschmidt, 1995 and the reference list in SH).

Theoretically, if one knew the historical circulation patterns for certain consecutive time periods then there would be no fundamental difficulty in solving the inverse problem: reconstruction of historical distributions of the sediment throughout the basin. In practice, however, this task is not as straightforward as one might expect. Yet recently some authors have addressed the issue, showing that the approach may be useful (*e.g.*, Sündermann and Klöcker, 1983; Bitzer and Pflug, 1990; see more references in SH).

In SH we studied the LGM circulation. Here we use the same threefold approach to address the MWE mode of the NA circulation in order to show how the method helps shed new light on sediment transport and deep-ocean ventilation in case of suppressed conveyor operation.

NUMERICAL MODELS AND COMPUTER EXPERIMENTS

We employ a planetary-geostrophic ocean circulation model especially designed for coarse-resolution, large-scale ocean circulation studies (fully described in Seidov (1996) and Seidov and Prien (1996)) as the major tool. This model is executed in the same manner as in Seidov *et al.* (1996) with the only difference of half the horizontal resolution used here to speed up computations (see SH for details). The sedimentation model in use here was designed by Haupt (1995) and tested in Haupt *et al.* (1994, 1995). The model was revised in SH to incorporate the impact of deep ventilating convection on settling particles. The water volume trajectory-tracing model was developed by Haupt (1995) and was employed to trace particle drifts in the northern North Atlantic (Haupt *et al.*, 1994, 1995). As in case of the sediment transport model, this trajectory-tracing model was revised in Seidov and Haupt (1997) for the convection impact. This model uses a hybrid Eulerian-Lagrangian, or semi-Lagrangian, approach with the velocity components given by the OGCM being interpolated to the positions of the Lagrangian particles from the nearby grid points of the Eulerian numerical grid.

The domain comprising a basin from 10°N to 80°N is adopted for simulations. These latitudinal limits are used because reliable sea surface salinity (SSS), arranged on a regular grid covering an extended area and suitable for numerical

modeling, is currently available only in the region north of 40°N. So, a compromise is made to extend the model domain to 10°N with a sponge layer at the southern boundary (Seidov *et al.*, 1996). However, the North Atlantic branch of the conveyor cannot be modeled without at least including the subtropical region. The ocean circulation is spun up from complete rest toward the equilibria relevant to modern and MWE surface boundary conditions under momentum and buoyancy forcing across the sea surface provided by specified annual mean wind stress, sea surface temperature (SST) and SSS.

The salinity conveyor belt is driven by convection and newly formed deep-water outflow at high latitude but convection itself occurs due to the cooling of warm and salty water brought by the conveyor from the subtropics. More detailed discussion on the use of regional versus global models is given in Seidov *et al.* (1996) and SH.

Numerical solutions to the OGCM equations are obtained on a regular numerical grid with $2° \times 2°$ horizontal resolution and 12 vertical levels unevenly spaced from the surface to the bottom depth at 4.6 km (on the details of discretization in space see SH).

The ocean circulation model is driven by the momentum flux specified by the wind stress at the sea surface and some "effective" heat and freshwater fluxes emerging in a pseudo-inverse runs employed in this study, as well as in a number of previous studies using this ocean circulation model (*e.g.*, Seidov, 1996; Seidov *et al.*, 1996; SH). In such 'inverse-flux' runs, temperature and salinity of the uppermost layer (at 50 m) are restored to the specified SST and SSS with a relaxation time of 50 days (Bryan, 1987). These boundary conditions imply that the heat and freshwater fluxes across the sea surface are such that would bring the upper ocean temperature and salinity to observed SST and SSS values within 50-days of e-folding time in the absence of all other processes in the upper layer (*e.g.*, advection, horizontal diffusion, etc.). Hence, these "effective" fluxes effect the sea surface climatology control over the uppermost level thermohaline structure yet do not equate them completely (see details in Bryan and Lewis, 1979; Sarmiento and Bryan, 1982; Bryan, 1987; Seidov, 1996). In the reference run, the surface climatology was extracted from Levitus (1982). The sea surface conditions for the MWE were assembled from different sources including CLIMAP (1991) SST updated by Schulz (1994) and Sarnthein *et al.* (1995) to the north of 50°N and SSS from Duplessy *et al.* (1991) and Seidov *et al.* (1996) (see Table I in Seidov *et al.*, 1996). Restoring boundary conditions are applied also at the southern boundary at 10°N. At the southern boundary, a relaxation time of 1 year was chosen for restoring temperature and salinity to their modern values. This restoration period increases rapidly northward with no further restoration applied north of 16°N. Longer relaxation time at the southern boundary and rapid

decrease of the sponge layer control over the subtropical circulation lessen the ambiguities imposed on the MWE solution because of the thermohaline structure in the deep layers retain modern characteristics at the MWE (the deficiency of the sponge layer technique in relation to a trade-off implied in regional circulation studies versus global ones are discussed in more detail in Seidov *et al.*, 1996). We do not expect the northern North Atlantic convection to be affected in any way by the sponge layer at the southern wall. The convection there is mostly controlled by freshwater impact which was overwhelmingly strong during the MWE. However, a word of caution should be issued here concerning the use of a sponge layer specifically, and a regional model in general.

Concerning the use of the annual sea surface climatology we must add that, in principle, late-winter values of SST and SSS would be more appropriate, since it is the winter mixed-layer T and S properties that determine the structure of the oceanic interior by inducing isopycnal outcrop. However, in view of the MWE SST and SSS being predominantly summer values, the only plausible solution is to rely on the annually-mean values in a comparative study like the presented here (see also a discussion in Seidov *et al.*, 1996).

Wind stress for both the modern and MWE are the newest release from the ECHAM-3/T42 atmospheric model, generated for paleoclimatic studies by the groups at Max-Planck Institute in Hamburg and at Bremen University (Lorenz *et al.*, 1996). This same wind stress is used for the LGM in SH and for MWE here.

All experiments with the sediment transport model are initialized with the same sediment properties (sediment sources, settling velocity of 0.05 cm s^{-1} = 43.2 m day^{-1} (Shanks and Trent, 1980), density and porosity of sediment, grain size, and sedimentological grain diameter, and form factor of sediment particles). The simulations were run over 1000 years. It is not possible to run the model to a steady state condition because of the forward integration (*e.g.*, the bottom slope changes in time affect the critical velocities, critical erosion and suspension velocity, and consequently the sediment transport itself). To take into account the eolian sediment input from the atmosphere, a small flux of about 1.0×10^{-13}g $cm^{-2}s^{-1}$ (= 0.0864 mg $m^{-2}day^{-1}$) is prescribed at the uppermost layer as in Haupt *et al.* (1994). The sediment input is specified homogeneously over the sea surface. We did not include any other source of sediment because our task is to infer the impact of circulation on the sediment transport which can be seen most clearly in slowly settling particles. Hence, the difference in between modern and past eolian sediment patterns indicate a change of the circulation pattern. For a realistic sediment mapping other sources should be included, which is a task for another study which have not been done yet. After settling, the eolian sediment is also available at the sea floor (the sediment particles can re-enter the sediment flow through turbulent entrainment).

The trajectory-tracing model has been run over 500 years of model time using the steady state velocity field provided by the OGCM. The water parcels have no inherent settling velocity (that is they are neutrally buoyant) and, therefore, they move together with the water flow.

RESULTS

The present-day and the MWE simulated velocity fields may be inspected in Seidov *et al.* (1996). One may infer from these maps that the modern and meltwater paleo-circulation patterns are indeed very distinct, both in the upper and the deep ocean. The most noticeable feature of the upper meltwater ocean currents is the deviation of the paleo-North Atlantic Drift from its modern north-eastern path (which is also found in the LGM case) and a reversed Norwegian Current in the NGS (which is a MWE-specific feature). Moreover, total meridional overturning reveals reversed overturning (which means a cyclonic meridional streamfunction as seen from east to west in the vertical plan) in the upper ocean down to 1 km and to the north of 40°N. The MWE convection pattern shows no convection to the north of 50°N and much shallower convection between 40°N and 50°N in the central and eastern part of the ocean (see Figure 5 in Seidov *et al.* (1996)). There is a strong incursion of Antarctic Bottom Water (AABW), dominating the abyssal-to-deep ocean during the MWE because of virtually non-existent NADW production at that time. This is in a good agreement with the water mass contouring by Sarnthein *et al.* (1994).

There is a much stronger difference between the MWE and modern circulation structures than between the LGM and the modern ones. However, one particular feature which makes the LGM and MWE deep ocean circulation more similar to each other than to the modern one in the western subtropical area, namely that both paleo patterns lack a strong deep western boundary current.

Today's southward deep return current is a deep-ocean western boundary flow forming a strong counter-current under the Gulf Stream. This western boundary current is well recognized as the most prominent feature of the thermohaline circulation (Stommel and Arons, 1960). Though a noticeably weaker western boundary current still existed at the LGM, the descending branch returned to the south-western basin, largely as a broad zonal westward flow in the middle latitudes. At the MWE, there is further degradation of the deep western boundary current. Instead of this southward boundary flow there is an increased incursion of AABW flowing northward at much shallower depths than at present.

Hence the re-deposited sediment in the eastern mid-to-high latitudes might be of different origin. Today, the drifts indicate the transport of material largely from north-east to west and south-west. In contrast, during the MWE some drifts could

change direction of transport to re-deposit the grains from south to north and north-west. Note that because of the coarse resolution we are not able to reproduce accurately the spatial boundaries between the drifts. We can only give a general picture of sediment drifts where sedimentation rates are noticeably higher than elsewhere in the basin.

Total accumulation is governed by the requirement that sources and sinks must balance at the sea surface and are the same for both time periods. The spatial distribution of modern and meltwater sediment is, however, different and reveals two distinctly different circulation modes between present and the MWE. A very high accumulation rate associated with the present-day mode of circulation is found in the vicinity of Iceland in the Irminger Basin, along the Reykjanes Ridge at both the south and north sides of Iceland, at the Rockall Plateau and in the NGS (Fig. 1a). This is in agreement with the present-day concept of sediment trapping in these areas (McCave and Tucholke, 1986; Bohrmann *et al.*, 1990). We find that the modeled sediment accumulation rates are smaller than those which have been measured. This is because of the low eolian sediment input from the top, and also because of the missing lateral input (Haupt, 1995). The sediment is transported by the deep western southward boundary current with local maxima near Newfoundland and further to the south in and near the Caribbean (McCave and Tucholke, 1986). We note that Iceland and the Caribbean are represented by seamounts in the model bottom topography; hence the non-zero accumulation rates are artifacts at the exact positions of these islands.

As the meltwater North Atlantic Current diverged from today's north-eastern path, the accumulation rate in the Iceland and Irminger Basins dropped and a significant part of the sediment mass was spread over the abyssal plain in the Canary Basin (Fig. 1b). Here we have a clear indication of the very strong impact of the circulation on the pelagic sediment in this area caused by essential change of the inflow/outflow and the convection regime in the northern NA and Nordic Seas. Note that although the sedimentation rate is far lower there than in the Iceland Basin, the sediment mass is roughly the same because bottom area in the latitude/longitude grid cells increases rapidly to the south. The sedimentation rate around Iceland decreased by over a factor of two as compared with its modern value (compare Figs. 1a and 1b). This is mainly because of the absence of ventilating convection both in the NGS and in the Irminger Sea. At the LGM, a relatively high glacial accumulation rate still emerges in the model in the Newfoundland Basin (SH). However, we do not see continuous southward sediment transport along the North American coast, a signature of all our experiments based on the modern ocean surface climatology. Instead, a noticeable southward sediment transport is found at the eastern flank of the Mid-Atlantic Ridge. At the MWE this tendency is increased significantly. The accumulation rate in the

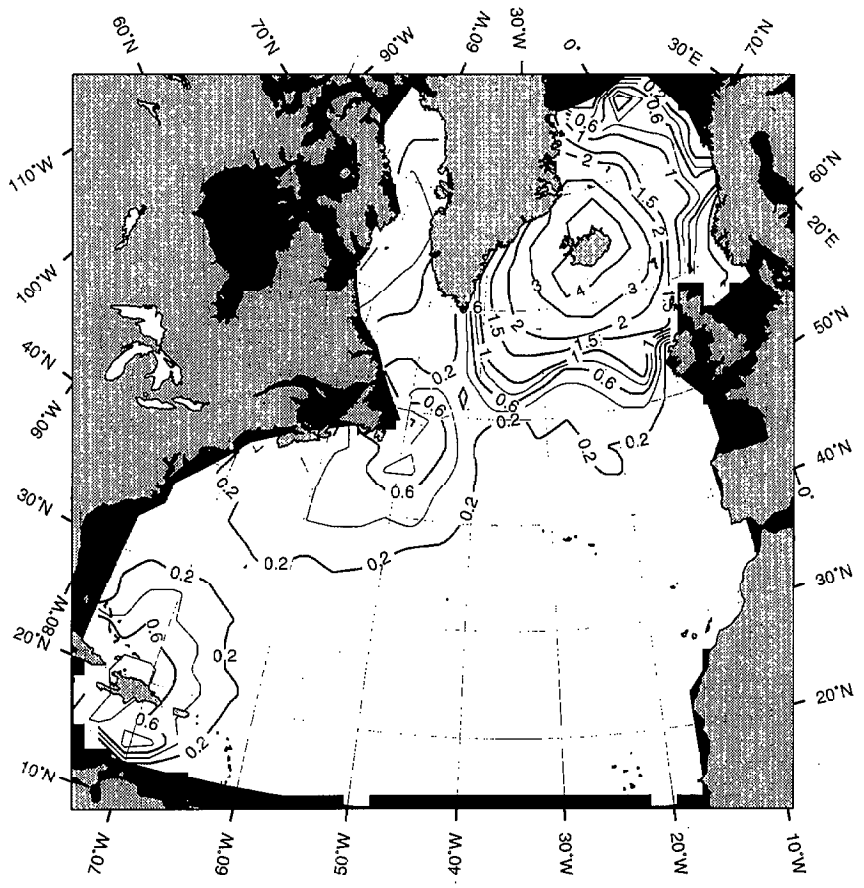

FIGURE 1a Sedimentation rate (cm/1000 yr.) produced by the modern ocean circulation patterns.

Newfoundland Basin decreased in comparison with the LGM run, whereas deposition was stronger at the eastern flank of the Mid-Atlantic Ridge. The area between Newfoundland and the Caribbean is almost totally free of sediment deposition.

Although most of the features common to the two sediment transport patterns (the modern and the MWE) can be explained by comparing them with the horizontal circulation patterns given by velocity vector maps, fundamental differences between modern, glacial and meltwater ventilation and sedimentation regimes are not revealed using solely the velocity maps. The transport in a transit area of intense ventilation can differ principally depending on whether convection is taken into account or ignored. The actual motion of water is masked in traditional

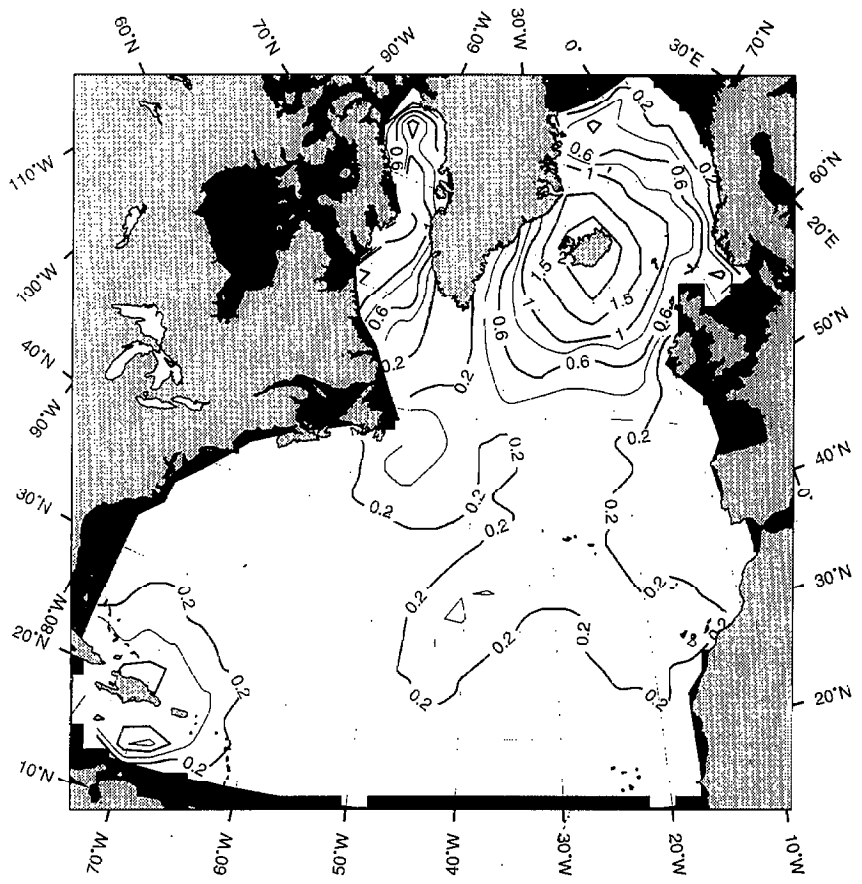

FIGURE 1b Sedimentation rate (cm/1000 yr.) produced by the MWE ocean circulation patterns.

Eulerian calculations and mappings because of 'invisible' vertical motion, both in the three-dimensional flow and especially in the convective 'chimneys' (for more details see discussion in SH).

In the discussed experiments, the particles visualizing the flow were deployed in different areas. In each of the areas, about 30 particles started to travel through the Eulerian velocity fields, once each in the modern and in the MWE cases. In SH we employed two different techniques to show the trajectories. First, all trajectories were shown as colored 'spaghetti' to delineate the depth of a particle. Another technique depicts only two pairs of trajectories but shows the elapsed time and the water parcel depth along the trajectories. Here we use the same visualization technique which shows the particles' pathways with depth and

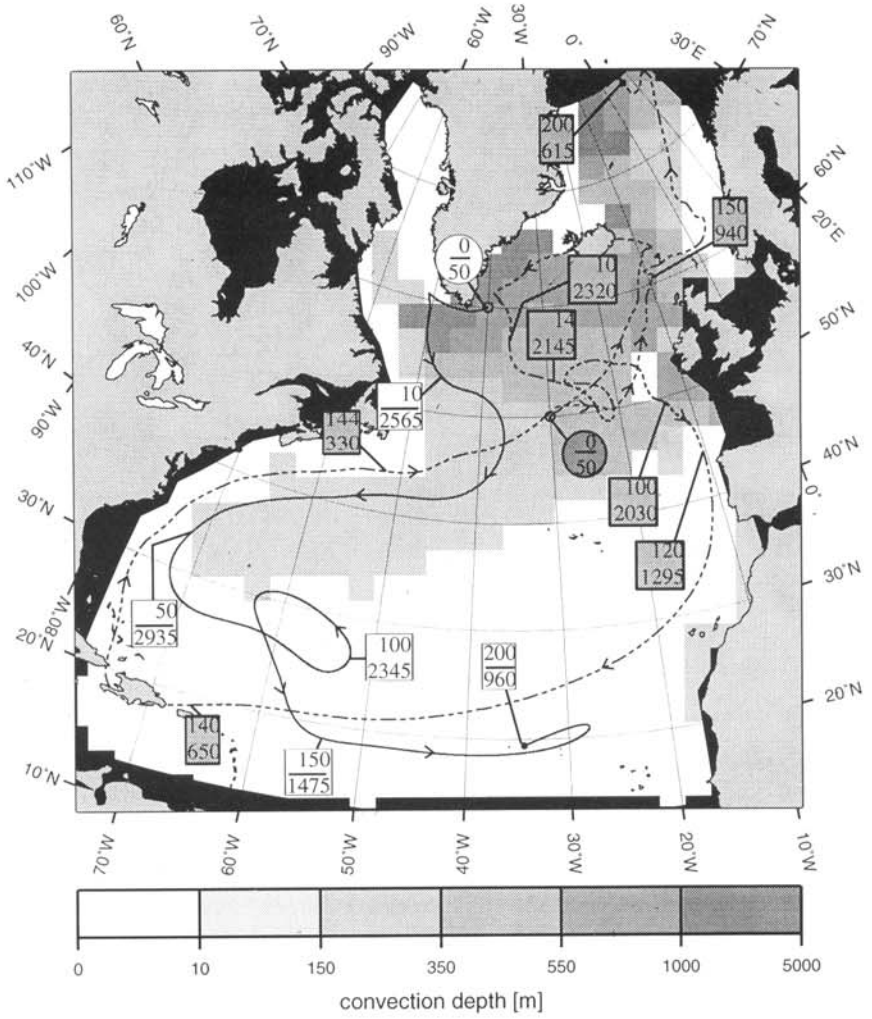

FIGURE 2a 200-year history of pairs of the Lagrangian particles for modern. Small rectangles show elapsed time and depth; small circles indicate starting points, the arrows show the direction of motion, and the bullets indicate the end points of the trajectories. One of the trajectories of each pair is presented by broken line. The convection depths are shown by different shades of gray.

elapsed time shown in small rectangles attached to the trajectories (Figs. 2a-d). Although the model time in the trajectory-tracing calculations was over 500 years, only the tracks for the first 200 years of the elapsed time are shown in the maps to avoid confusion. The upper panel (Fig. 2a, b) depicts the present day motion, whereas the lower panel (Fig. 2c, d) shows the trajectory at the MWE. A striking

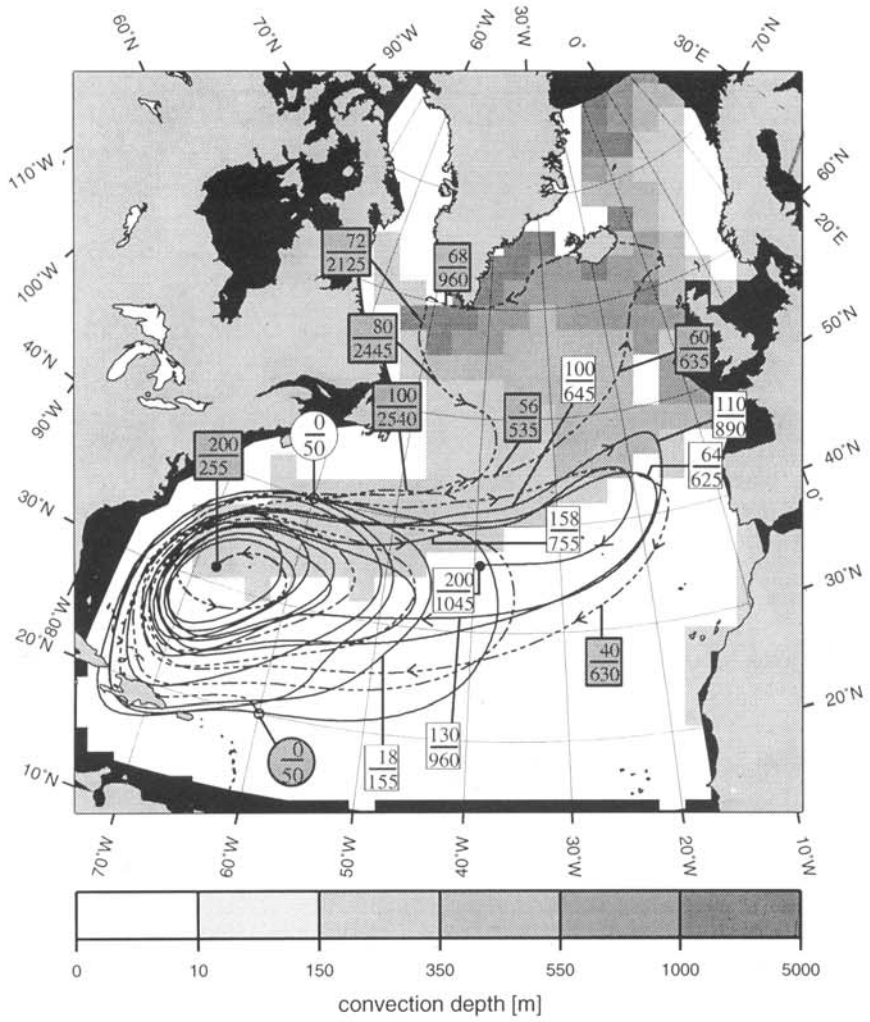

FIGURE 2b 200-year history of pairs of the Lagrangian particles for modern. Small rectangles show elapsed time and depth; small circles indicate starting points, the arrows show the direction of motion, and the bullets indicate the end points of the trajectories. One of the trajectories of each pair is presented by broken line. The convection depths are shown by different shades of gray.

feature of the trajectory map is the change in the meltwater deep-ocean circulation regime which would not be so obvious from the velocity maps shown in Seidov *et al.*, (1996). Note that there are particles deployed in the convection regions in both cases. However, at the MWE, no particles penetrated into the deep ocean, regardless of where they started their journey. Note that in a coarse resolution

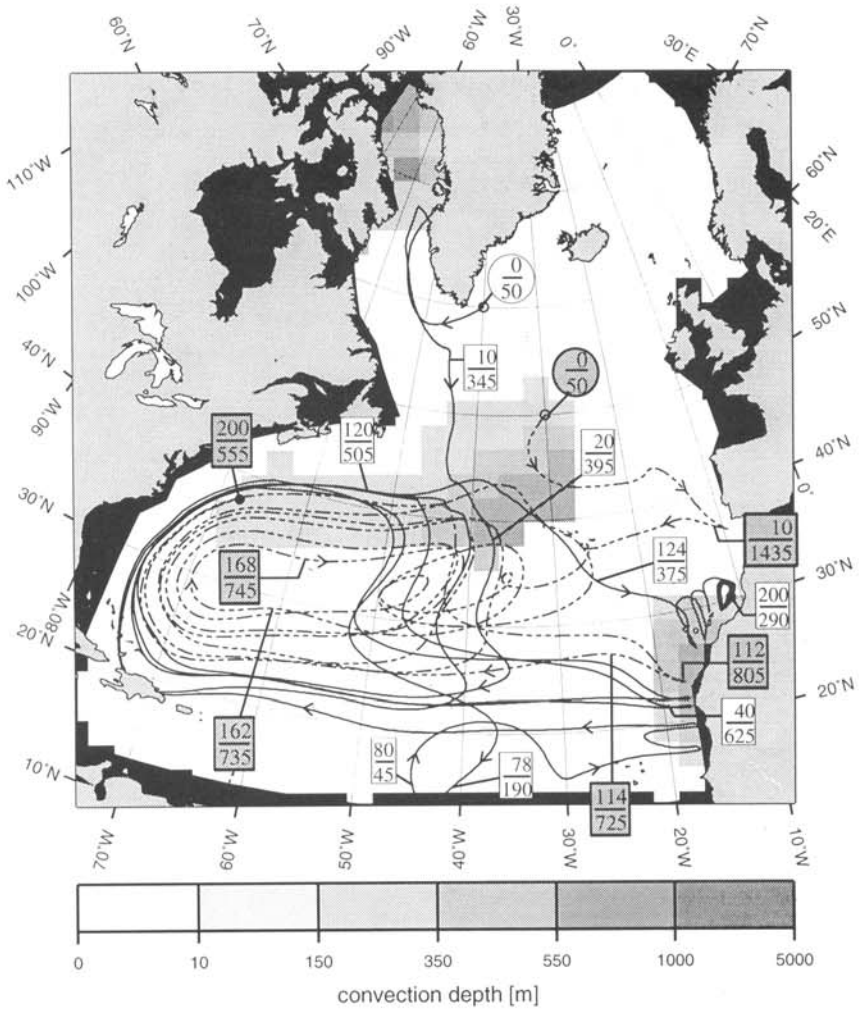

FIGURE 2c 200-year history of pairs of the Lagrangian particles for MWE. Small rectangles show elapsed time and depth; small circles indicate starting points, the arrows show the direction of motion, and the bullets indicate the end points of the trajectories. One of the trajectories of each pair is presented by broken line. The convection depths are shown by different shades of gray.

model it is impossible to simulate accurately the Denmark Strait overflow, the fluid parcels in the model, after entering the NA through the Denmark Straits, descend through convectively mixing chimneys rather than within a waterfall density current. This deficiency is common to many OGCMs and is though to have some impact on the net formation rate and structure of NADW (*e.g.*, Roberts

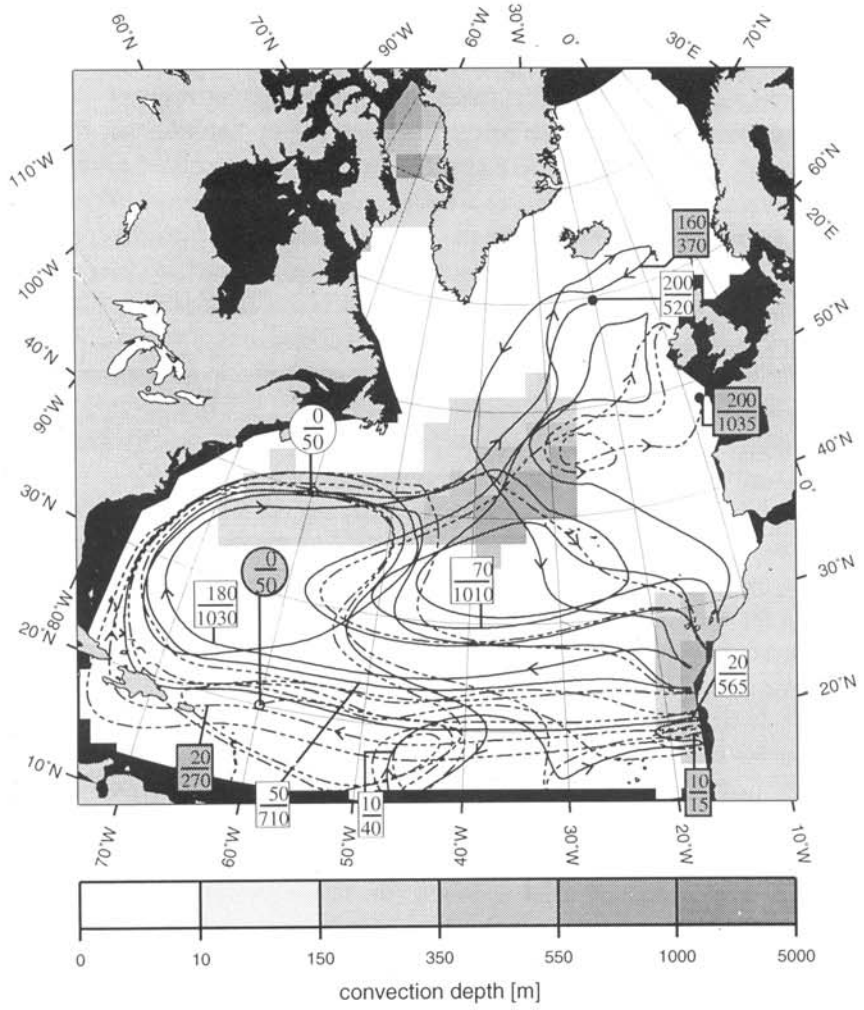

FIGURE 2d 200-year history of pairs of the Lagrangian particles for MWE. Small rectangles show elapsed time and depth; small circles indicate starting points, the arrows show the direction of motion, and the bullets indicate the end points of the trajectories. One of the trajectories of each pair is presented by broken line. The convection depths are shown by different shades of gray.

et al., 1996). However, in our study this impact is not as important as it might be expected. Firstly, we study a case of complete cessation of NADW due to convection capping during the MWE, and therefore the secondary effect of the overflow not modeled accurately may not decisively hamper our simulations. Secondly, the parcels descending to the deeper ocean within the density currents

and sliding along the outcropped isopycnals in the convection zones all reach the westward-southwestward deep flow, and therefore cannot be distinguished in their further travel within the deep ocean.

With respect to the fate of the descending particles, color maps of particles trajectories may help to trace the parcels after entering the North Atlantic through the Denmark Straits. As in SH, in Figure 3 the trajectories are colored to show the depth of a particle (convection sites are depicted by different shades of gray: the deeper the convection, the darker the shade). We use the sunlight spectrum colors, from dark red in the uppermost layer (<100 m) to violet and black in the two deepest layers, to visualize vertical migration of the water parcels. Although the model time in the trajectory-tracing calculations was over 500 years, only the tracks for the first 100 years of the elapsed time are shown in the maps to avoid confusion.

A comparison of the modern and MWE trajectories (Figs. 3 a and b) reveals the fundamental difference of water transport during these two time slices. Present day southward flow in the deep western boundary current is the dominant feature of the deep ocean conveyor and conforms well to the Stommel-Arons theory. In contrast, the MWE trajectories indicate that at that time slice there were no ventilation of the deep ocean in the NA at all (Fig. 3b), and therefore one cannot find any indication of the deep ocean conveyor in the NA. The spaghetti of the MWE trajectories indicate also that the Nordic Seas were rather isolated area at that time. The selected trajectories illustrate the collapse of the forward conveyor and delineate the shallow and slow motion within the upper ocean layers.

Hence, on the basis of the spaghetti maps and the trajectories in Figure 2, deep water production is found nowhere in the MWE North Atlantic. We note that Figure 2c, d shows that water ventilation of subsurface and intermediate water still occur to the south of 40°N. However, the fate of descending volumes are quite different to what occurs in the present-day simulations. This descended water limits the subtropical warm and salty pool of high potential vorticity water to the western part of the basin and upwells within this pool and western boundary layer (Fig. 2c, d). The eastern upper-to-intermediate water move largely southward and comprises the reverse upper-ocean conveyor (Seidov *et al.*, 1996). The color map in Fig. 3b also indicates that there was still quite intensive ventilation of the subtropical thermocline, which is an inherent feature of wind-driven circulation in the subtropics and therefore not affected by the high-latitudinal convection regime. However, the ventilation regime in the subtropics was essentially different from the present-day regime. At the MWE, the subtropical thermocline is ventilated not only from the north, but largely from the east, which makes it decisively different from its modern analogue. Indeed, the density outcrop to the north and east of the Ekman-induced pool of high potential vorticity leads to

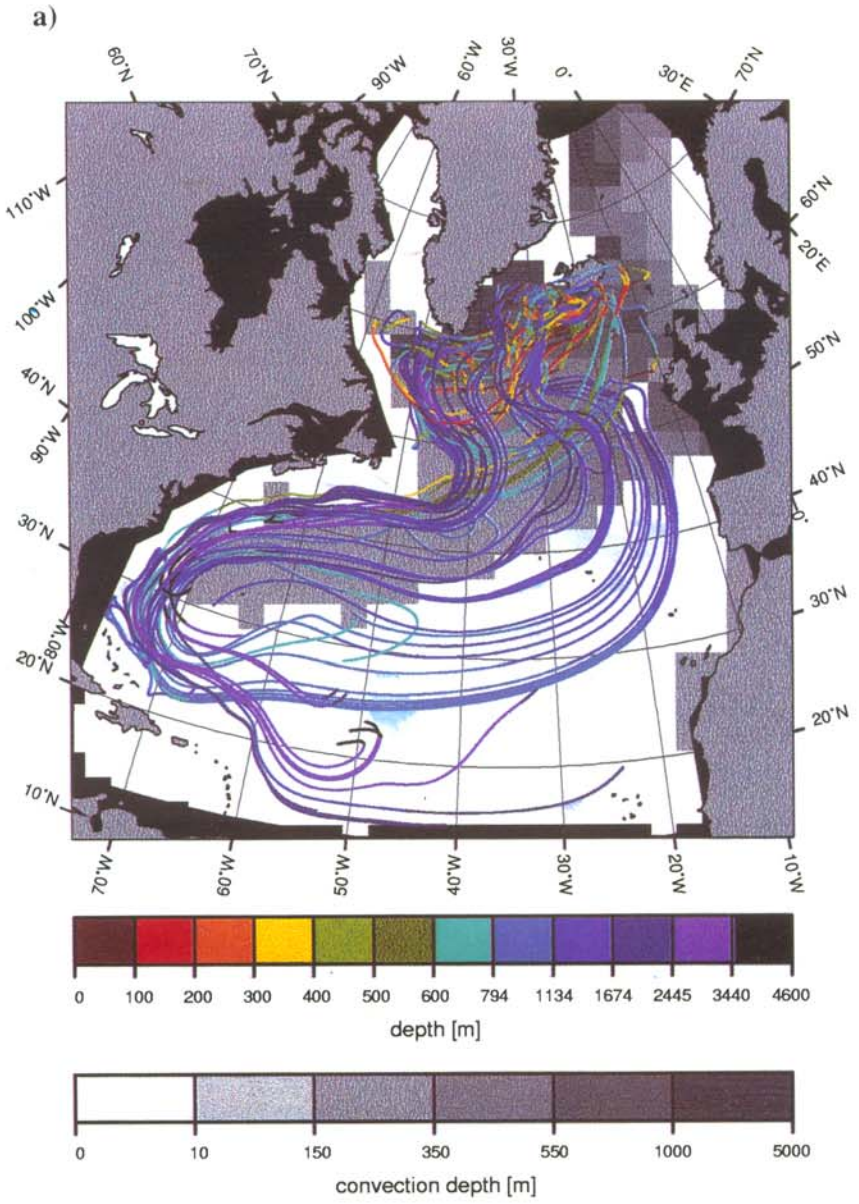

FIGURE 3 Spaghetti of particle trajectories deployed at the HM in the central part of the northern North Atlantic: a) Present-day; b) MWE. The convection depths are shown by different shades of gray. First 100 years of the particles history are shown. The depth is indicated by colors from the color palette; as a particle descends or upwells the color of the trajectory changes.

b)

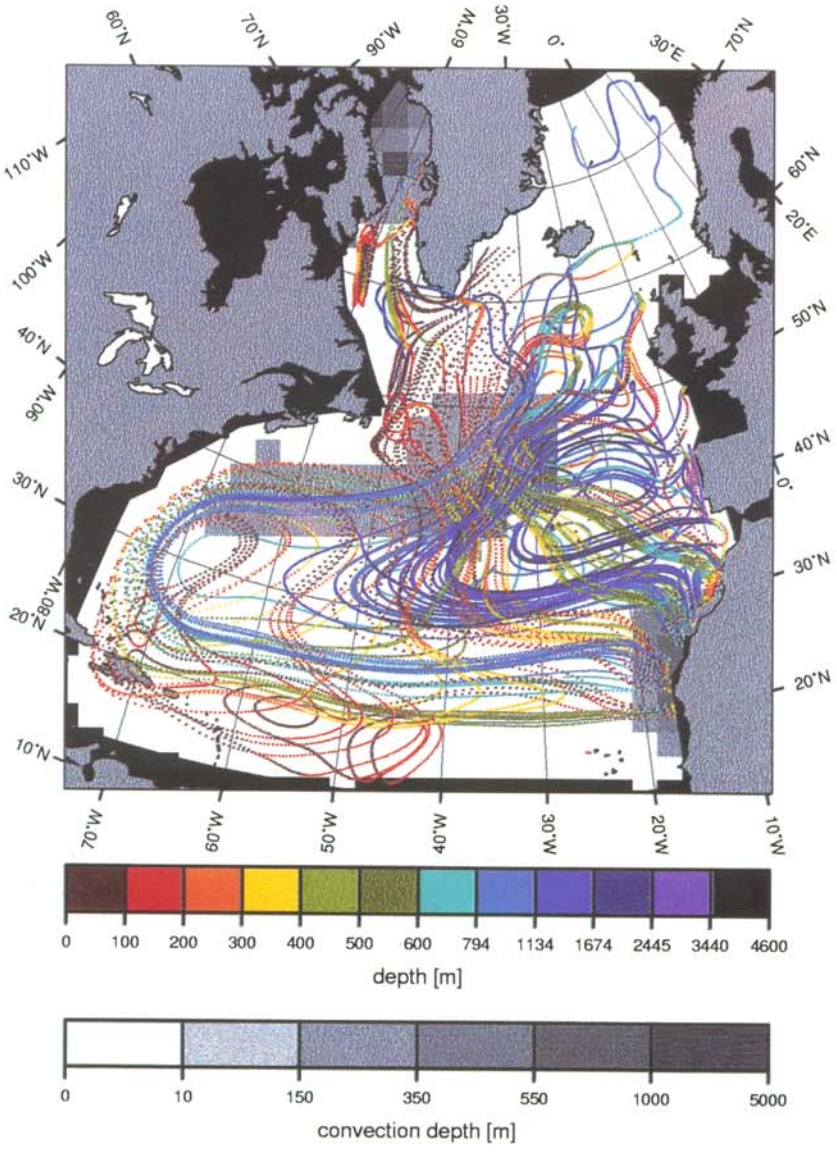

FIGURE 3 *(Continued).*

separation of this pool from the eastern boundary, which in turn leads to collapse of the North Atlantic Drift and eventually to suppression of the thermohaline conveyor.

DISCUSSION AND CONCLUSIONS

A threefold modeling approach was employed to understand particular aspects of the meltwater paleoceanography of the North Atlantic. Primary among those are the ventilation regime in the North Atlantic. The threefold approach helps to reduce ambiguity of the traditional circulation modeling and data analysis. There are some reasons why such ambiguity may arise.

Commonly, assumed features of a water flow, thought to be suitable for explaining a particular distribution of proxy data, are largely based on speculations. There is no guarantee that this hypothetical flow would satisfy hydrodynamic restrictions posed over the ocean by the wind stress, ocean geometry, bottom morphology, and heat and freshwater sea surface fluxes. OGCMs may prove a useful addition to analyze the proxy data, having a reasonable and hydrodynamically consistent circulation pattern. Still, it would be better to validate this pattern on the basis of data not used to constrain the conditions driving the OGCM. Here we employ a sediment transport model to provide such means. Having simulated a sedimentation pattern one can validate the resulting circulation pattern by comparison with existing interpretations of the sediment structures. As pelagic (and to some extent hemi-pelagic) sediments can be used to verify computations of the modern deep-ocean current, they can also be employed to certify paleo-circulation.

Based on only partly known SSS, recently corrected SST, and simulated glacial wind stress, we have arrived at results which largely conform to current ideas about ventilation and overturn in the North Atlantic at the height of a meltwater event subsequent to the last major glaciation. The sediment transport model output contains features that agree well with interpretation of sediment data in the northern North Atlantic.

In the eastern part, our sediment model agrees with data that indicate increased flow along the eastern flank of the Mid-Atlantic Ridge. Dowling and McCave (1993) and Robinson and McCave (1994) provide evidence that the Feni Drift was substantially enhanced at the LGM. These authors interpret enhanced bottom current activity in the Rockall Trough region as an indicator of enhanced deep water production there. Though here we model the MWE pattern, the cessation of the deep western boundary current is common to both the LGM and MWE patterns. Our results, indicating a south-west shift of convection that facilitated

only the intermediate water production at the MWE, are in good agreement with findings of Sarnthein *et al.* (1995).

Our trajectory-tracing model reveals very different fates of the water volumes in the modern and LGM cases. The lack of NADW production in the MWE North Atlantic is strongly supported by the proxy data (Sarnthein *et al.*, 1994, 1995).

Based on a threefold numerical simulation of the NA circulation and sedimentation we conclude the following:

1. Sedimentation in the NA is non-linearly coupled to the circulation modes associated with different surface climatology. The MWE sedimentation pattern differs fundamentally from the modern sedimentation pattern showing a strong decrease of sediment deposition rate in the vicinity of Iceland, an increase of sedimentation rate in the eastern NA, and a dramatic drop in sedimentation rate in the Gulf Stream area, if compared to the present-day rates in these regions.

2. The results suggest practically absent MWE sediment deposition in the Gulf Stream area, and a lower rate than at present in the Caribbean.

3. The trajectory-tracing model indicates complete absence of the deep ocean ventilation at the MWE. The model reveals disappearance of the deep western boundary current and westward contraction of the subtropical warm pool. This contraction leads to collapse of the eastern continuation of the North Atlantic drift and contributes to formation of the upper ocean reverse conveyor.

Acknowledgements

The authors gratefully acknowledge the help and support given by Michael Sarnthein and Karl Stattegger. We are very grateful to Avan Antia who helped to improve the language and style of the manuscript. The comments given by an anonymous reviewer are gratefully acknowledged. This study was supported by the Deutsche Forschungsgemeinschaft (DFG) within the framework of the SFB 313 at Kiel University (SFB 313 Project B4) and by the German National Program of Climate Research.

References

Bitzer, K. and Pflug, R. DEPOD: (1990) A three-dimensional model for simulating classic sedimentation and isostatic compensation in sedimentary basin. In *Quantitative Dynamics Stratigraphy*, T. A. Cross (ed.), pp. 335–348, (Prentice Hall, New York).

Bohrmann, G., Henrich, R. and Thiede, J. (1990) Miocene to Quaternary paleoceanography in the northern North Atlantic: Variability in carbonate and biogenic opal accumulation. In *Geological history of the polar oceans: Arctic versus Antarctic*, U. Bleil, and J. Thiede (eds.), pp. 647–675, (Kluwer Academic Publ., Dordrecht).

Bond, G., Heinrich, H., Broecker, W., Labeyrie, L., McManus, J., Andrews, J., Huon, S., Jantschik, R., Clasen, S., Simet, C., Tedesco, K., Klas, M., Bonani, G. and Ivy, S. (1992) "Evidence for massive discharges of icebergs into the North Atlantic ocean during the last glacial period," *Nature*, **360**, 245–249.

Boyle, E. A. and Keigwin, L. D. (1987) "North Atlantic thermohaline circulation during the past 20,000 years linked to high-latitude surface temperature," *Nature*, **330**, 35–40.

Broecker, W. (1991) "The great ocean conveyor," *Oceanography*, **1**, 79–89.

Broecker, W. S. and Denton, G. H. (1989) "The role of ocean atmosphere reorganizations in glacial cycles," *Geochim. Cosmochim. Acta*, **53**, 2465–2501.

Bryan, F. (1986) "High-latitude salinity effects and interhemispheric thermohaline circulations," *Science*, **323**, 301–304.

Bryan, F. (1987) "Parameter sensitivity of primitive equation ocean general circulation models," *J. Phys. Oceanogr.*, **17**, 970–985.

Bryan, K. and Lewis, L. J. (1979) "A water mass model of the world ocean," *J. Geophys. Res.*, **84**, 2503–2517.

Climate: Long-Range Investigation Mapping and Prediction (CLIMAP) Project Members (1981) Seasonal reconstructions of the Earth's surface at the Last Glacial Maximum, *Map and Chart Ser. MC-36*, pp. 1–18, Geol. Soc. of Am., Boulder, Colo.

Dowling, L. M. and McCave, I. N. (1993) "Sedimentation on the Feni drift and late Glacial bottom water production in the northern Rockall Trough," *Sed. Geol.*, **1993**, 79–87.

Duplessy, J.-C., Labeyrie, L., Julliet-Lerclerc, A., Duprat, J. and Sarnthein, M. (1991) "Surface salinity reconstruction of the North Atlantic ocean during the last glacial maximum," *Oceanol. Acta*, **14**, 311–324.

Fichefet, T., Hovine, S. and Duplessy, J.-C. (1994) "A model study of the Atlantic thermohaline circulation during the last glacial maximum," *Nature*, **372**, 252–255.

Goldschmidt, P. (1995) "Accumulation rates of coarse-grained terrigenous sediment in the Norwegian-Greenland Sea: Signals of continental glaciation," *Mar. Geol.*, **128**, 137–151.

Goldschmidt, P. M., Pfirmann, S., Wollenburg, I. and Henrich, R. (1992) "Origin of sediment pellets from the Arctic Seafloor. Sea ice or icebergs?," *Deep Sea Res.*, **372**, 252–255.

Gordon, A. (1986) "Interocean exchange of thermocline water," *J. Geophys. Res.*, **91**, 5037–5046.

Haupt, B. J. (1995) *Numerische Modellierung der Sedimentation in nördlichen Nordatlantik, Ber. SFB 313, Univ. Kiel*, **54**, 1–129.

Haupt, B. J., Schäfer-Neth, C. and Stattegger, K. (1994) "Modeling sediment drifts: A coupled oceanic circulation-sedimentation model of the northern North Atlantic," *Paleoceanogr.*, **9**, 897–916.

Haupt, B. J., Schäfer-Neth, C. and Stattegger, K. (1995) "Three-dimensional numerical modeling of Late Quaternary paleoceanography and sedimentation in the northern North Atlantic," *Geol. Rdsch.*, **84**, 137–150.

Honjo, S. (1990) Particle fluxes and modern sedimentation in the Polar Oceans. In *Polar Oceanography, Part B*, W. O. Smith (ed.), pp. 687–739, (Acad. Press, Boston, Massachusetts).

Levitus, S. (1982) Climatological Atlas of the World Ocean. NOAA Prof. Pap., pp. 173.

Lorenz, S., Grieger, B., Helbig, Ph. and K. Herterich, K. (1996) "Investigating the sensitivity of the Atmospheric General Circulation Model ECHAM 3 to paleoclimate boundary conditions," *Geol. Rdsch.*, **85**, 513–524.

Manabe, S. and Stouffer, R. J. (1988) "Two stable equilibria of a coupled ocean-atmosphere model," *J. Climate*, **1**, 841–866.

Manabe, S. and Stouffer, R. J. (1995) "Simulation of abrupt change induced by freshwater input to the North Atlantic Ocean," *Nature*, **378**, 165–167.

Marotzke, J. and Willebrand, J. (1991) "Multiple equilibria of the global thermohaline circulation," *J. Phys. Oceanogr.*, **21**, 1372–1385.

McCave, I. N. and Tucholke, B. E. (1986) Deep current controlled sedimentation in the western North Atlantic. In *The Geology of North America*, vol. M., The Western North Atlantic Region, P. R. Vogt and B. E. Tucholke, (eds.) pp. 451–468, (The Geological Society of America, New York).

Rahmstorf, S. (1994) "Rapid climate transitions in a coupled ocean-atmosphere model," *Nature*, **372**, 82–85.

Rahmstorf, S. (1994) "Bifurcations of the Atlantic thermohaline circulation in response to changes in the hydrological cycle," *Nature*, **378**, 145–149.

Roberts, M. J., Marsh, R., New, A. L. and Wood, R. A. (1996) "An intercomparison of a Bryan-Cox-type ocean model and an isopycnic ocean model. Part 1: the subpolar gyre and high-latitude processes," *J. Phys. Occanogr.*, **26**, 1495–1527.

Robinson, S. G. and McCave, I. N. (1994) "Orbital forcing of bottom-current enhanced sedimentation on Feni Drift, NE Atlantic, during the mid-Pleistocene," *Paleoceanogr.*, **9**, 943–972.

Sarmiento, J. L. and Bryan, K. (1982) "An ocean transport model for the North Atlantic," *J. Geophys. Res.*, **87**, 394–408.

Sarnthein, M., Winn, K., Jung, S. J. A., Duplessy, J. C., Labeyrie, L., Erlenkeuser, H. and Ganssen, G. (1994) "Changes in East Atlantic deepwater circulation over the last 30,000 years—8 time slice reconstructions," *Paleoceanogr.*, **9**, 209–267.

Sarnthein, M., Jansen, E., Weinelt, M., Arnold, M., Duplessy, J.-C., Erlenkeuser, H., Flatoy, A., Johannessen, G., Johannessen, T., Jung, S., Koc, N., Labeyrie, L., Maslin, M., Pflaumann, U. and Schulz, H. (1995) "Variations in Atlantic Ocean paleoceanography, 50°–85°N: A time-slice record of the last 300,000 years," *Paleoceanogr.*, **10**, 1063–1094.

Schmitz, W. J. Jr. (1995) "On the interbasin-scale thermohaline circulation," *Rev. Geophys.*, **33**, 151–173.

Schulz, H. (1994) *Meeresoberflächentemperaturen im frühen Holozän 10,000 Jahre vor heute*, Ph.D. Dissertation, Universität Kiel, Kiel, Germany.

Seibold, E. and Berger, W. H. (1993) *The sea floor; an introduction to marine geology*, 2nd ed., (Springer-Verlag, New York).

Seidov, D. (1996) "An intermediate model for large-scale ocean circulation studies," *Dyn. Atm. Oceans*, **25**/1, 25–55.

Seidov, D. and Haupt, B. J. (1997) "Simulated ocean circulation and sediment transport in the North Atlantic during the last glacial maximum and today," *Paleoceanogr.*, **12**, 281–305.

Seidov, D. and Prien, R. (1996) "A coarse resolution North Atlantic ocean circulation model: an intercomparison study with a paleoceanographic example," *Ann. Geophys.—Atmosph. Hydrosph. & Space Sci.*, **14**, 246–257.

Seidov, D., Sarnthein, M., Stattegger, K., Prien, R. and Weinelt, M. (1996) "North Atlantic ocean circulation during the Last Glacial Maximum and subsequent meltwater event: A numerical model," *J. Geophys. Res.*, **110/C7**, 16,305–16,332.

Shanks, A. L. and Trent, J. D. (1980) "Marine snow: Sinking rates and potential role in vertical flux," *Deep Sea Res*, **27A**, 137–143.

Stocker, T. F. (1994) "The variable ocean," *Nature*, **367**, 221–222.

Sündermann, J. and Klöcker, R. (1983) Sediment transport modeling with applications to the North Sea. In *North Sea Dynamics*, pp. 453–471, (Springer-Verlag, New York).

Weaver, A. J. and Hughes, T. M. C. (1994) "Rapid interglacial climate fluctuations driven by North Atlantic ocean circulation," *Nature*, **367**, 447–450.

Wright, D. and Stocker, T. F. (1991) "A zonally averaged ocean model for the thermohaline circulation. Part I: Model development and flow dynamics," *J. Phys. Oceanogr.*, **21**, 1713–1724.